Vol. 4, No. 3, pp. 169-192, (June 2023)
DOI: 10.21608/aujes.2023.208949.1148
Aswan University Journal of Environmental Studies (AUJES)
Online ISSN: 2735-4237, Print ISSN: 2735-4229
Journal homepage: https://aujes.journals.ekb.eg/ E-mail: AUJES@aswu.edu.eg
Original research

Optimization of total hardness removal efficiency of industrial wastewater using novel adsorbing materials

Mohamed F. Soliman[1 *], Mahitab Nazem M.[1], Ali A.M. Gad[2], Ali M. Ibrahim[3]

[1]Aswan University, Faculty of Engineering, Civil Engineering Department, Aswan, 81542, Egypt,
[2]Assuit University, Faculty of Engineering, Civil Engineering Department, Assuit, 71515, Egypt,
[3] Aswan University, Faculty of Science, Physics Department, Aswan, 81528, Egypt

Received: 4/5/2023 Accepted: 16/6/2023

Abstract:

One of the contaminants of industrial wastewater is hardness, which has harmful effects on our environment when discharge to surface water. Hence, various treatment methods have been studied to remove the hardness of wastewater. Herein, a series of oxide glasses with different compositions were prepared as novel adsorbents to dispose of hardness from industrial wastewater via adsorption treatment technique. It is found that the treatment with borosilicate glass (25% B_2O_3–20% SiO_2 – 5% CuO – 5% Bi_2O_3 – 45% Na_2O) exhibits the highest hardness removal efficiency. Based on such sample, the boundary conditions, including contact time, temperature, and adsorbent dosage are controlled to obtain the optimum removal efficiency. The optimum boundary conditions are found to be 150 min, and 15g L^{-1} for contact time, and adsorbent dosage, respectively. Fortunately, the efficiency is unaffected by the temperature of the adsorption process, which indicates no required expended energy and low cost water treatment. The effect of initial hardness concentration and pH of wastewater shows an initial increase in the removal efficiency to a maximum value at 150 mg L^{-1} and 6.5 – 7.2, respectively. The results from the contact time study were simulated by Langmuir and Freundlich isothermal adsorption models, and well fitted. Finally, the comparison with the previous studies shows that the experimental results exhibit excellent and acceptable hardness removal efficiency at the appropriate contact time and adsorbent dosage.

Keywords: hardness, adsorbent, borosilicate glass, oxide glass, adsorption process.

1- Introduction

Wastewater must pass through treatment stages before reuse or final disposal, and even drinking water not used directly but is exposed to pass through treatment stages. There are products have a great importance, which leads to the need to establish factories, such as: chemical and metal products, agriculture fertilizers, plastic productions, and explosive materials. The industrial wastewater of those factories contains hardness (Ambaye et al., 2021; Crini and Lichtfouse, 2019; Shahedi et al., 2020).

Corresponding author*: E-mail address: mohamed.soliman@aswu.edu.eg

Ranges of hardness in water are determined based on calcium carbonate concentration: less than 60 mg L^{-1} for soft water, 60–120 mg L^{-1} for middling hard water; 120–180 mg L^{-1} hard water, and more than 180 mg L^{-1} for very hard (Anesthesia et al., 2010). Water hardness is considered an effective parameter in water quality, which determines the appropriate use of water or a method of disposal. Jabbar-Lopez et al. (2021) reported that the hardness is the existent divalent ions, such as calcium, manganese, iron, and magnesium. Prevalent types for water hardness are calcium and magnesium as mentioned by Yan et al. (2008). Water hardness has a strong impact on health, Rapant et al. (2017) proved that infection of the Slovak population with diseases of oncological, gastrointestinal, and respiratory systems is attributed to groundwater hardness. Kozisek (2020) found that drinking water contaminated with magnesium leads to cardiovascular disease. Many other researchers studied the same point (Decundo et al., 2019; Kozisek, 2020; Rapant et al., 2017; Sharmin et al., 2020). The other hard water problem is that it causes deposits in household facilities and boilers, in addition to the bad effect of detergent cleaning performances (Bouassida et al., 2018; Suzuki et al., 2002). Several studies have used different methods of water hardness removal. Zereffa and Bekalo (2017) used a clay ceramic filter for water hardness removal; it could remove around 50 % of hardness. Halpegama et al. (2021) treated water by electrocoagulation (EC); its hardness removal efficiency was achieved to 63%. El-Nahas et al. (2020) used synthesis zeolitic materials as an adsorbent; its hardness removal efficiency was 90%. Wang and Lin (2019) treated water by Membrane Capacitive Deionization (MCDI), they achieved good results in removing Ca^{2+}. Capacitive Deionization (CDI) technology was used by Sun et al. (2021) to remove water hardness ions, and the removal efficiency of (CDI) reached more than 90%, that after five times of adsorption cycles. Hailu et al. (2019) conducted the ion exchange process by natural zeolite, and zeolite had a share in the removal of hardness. Ahn et al. (2018) reduced the water hardness by the carbonation process; they managed to remove 40–85% of the total hardness with this process. Kaur et al. (2021) prepared adsorbent by feedstock for water hardness, it was effective and low-cost as an adsorbent material. Among the used removal processes, adsorption was studied for adsorbing of ionic and atomic hardness species from water. Several researchers used this technique and studied the adsorbent efficiency of hardness removal. Adsorption is a surface phenomenon that works as adsorbent particles increase by contaminants adhering to the adsorbent particles' surface. Adsorbents' function is the attraction of contaminants molecules to stick to their atoms. The adsorption process is distinguished from other treatment methods in the following points: its simple design, it requires a small area for its implementation, and its initial cost is low. Various adsorbents were made, studied, and developed in previous studies, such as feedstock (Kaur et al., 2021), zeolite was synthesized from Ethiopian kaolin (Aragaw and Ayalew, 2019), synthetic nano-zeolites (Konale et al., 2020), bentonite (Kadir et al., 2017), kaolin-based geopolymer (Naghsh and Shams, 2017), kaolinite smectite (Es et al., 2019), hydrochloric acid activated natural kaolin (Wahyuni et al., 2021), coconut-shell (Of et al., 2022), activated charcoal from coconut shell (Jamilatun and Mufandi, 2020), coffee ground activated charcoal (Khaerul and Syahputri, 2021), banana stem charcoal (Mahyudin, 2019), grafted potato starch (Mgombezi and Vegi, 2020). The studied adsorbent in this research is oxide glasses, where oxide glasses are characterized by the presence of the dangling bonds, which may make them achieve success in the adsorption process. The oxide glasses may achieve the same performance as the previously studied adsorbents or outperform them. Vedishcheva and Wright (2014) reported that man synthesized glasses from 4000 years, and began studying glass structure in the 1920s after developing X-ray diffraction technique. Oxide glasses are useful in many applications and suitable to solve special problems because of their properties as mentioned by Axinte (2011). Axinte (2012) stated that the glasses

have an amorphous form; they are formed by the conventional melt quenching technique to the solid case without crystallization (Camilo et al., 2013; Jiménez et al., 2011). Yadav and Singh (2015) found that, forming of glass required a critical cooling rate. The aim of this study is reduce the concentration of the hardness, whatever water source, that to allow treated water to be used without exposure to the problems caused by hard water in terms of health problems when using it for drinking or problems when using it for other purposes. Where the World Health Organization stated that water containing a concentration of less than 60 mg L^{-1} of calcium carbonate is considered soft as reported by Takahashi and Imaizumi (1988), and this is what is expected to be reached. This study intends to investigate the optimum boundary conditions of the adsorption process by oxide glass, after reaching to an effective oxide glass formula. Finally, this research presents the influence of the wastewater sample properties on the adsorbent efficiency. The structural properties of the prepared oxide glasses were studied by XRD and FTIR spectra, as the structural properties play an important role in the efficiency of adsorbent.

2- Materials and Methods

2.1. Chemicals and wastewater samples

2.1.1 Chemicals

All chemicals are used in this study such as; Boron oxide B_2O_3, Silicon oxide SiO_2, Germanium oxide GeO_2, Phosphor oxide P_2O_5, Aluminum oxide Al_2O_3, Tin oxide SnO, Bismuth oxide Bi_2O_3, Copper (II) oxide CuO, Copper (I) oxide Cu_2O, Sodium carbonate Na_2Co_3, were obtained from Alfa Aesar, its purity was more than 99%.

2.1.2 Wastewater samples

In this study, wastewater samples were collected in the first experiment from the drainage of agricultural fertilizers manufactory and chemical industry, which was collected one day before the experimental work in June 2022. In the case of subsequent experiments, samples were synthesized. Synthesized wastewater samples have the same properties as original industrial wastewater samples in order to save the same conditions in all experiments. The wastewater samples have been collected or synthesized one day before the adsorption process, the samples were kept at 5^{o}C to experimental time, which matches with conditions mentioned by Torfs et al. (2016).

Synthesized samples are made by adding the required quantity of $CaCl_2$ and $MgSO_4.7\ H_2O$ into distilled water; this is to simulate the same Ca^{+2} and Mg^{+2} values in the initial sample of industrial wastewater and its pH value. The obtained samples have the initial concentration of total hardness 319 ± ٧ mg L^{-1} and pH 8.9, concentrations of Ca^{+2} and Mg^{+2} are 104 – 10٨ mg L^{-1} and 12.٦ – 1٣.٦ mg L^{-1} respectively. Analysis was carried out according to Standard Methods (APHA, 2002; Federation, 1999).

2.2. Oxide glasses definition

There are two different types of solid materials: crystalline and amorphous. The atomic arrangement in solid crystalline is regular; amorphous solid has an irregular atomic arrangement such as glass, ceramic, gel, and polymers. The types of glasses are oxide glasses and non-oxide glasses, oxide glass is composed of former, intermediate, and modifier. The former is the main ingredient in oxide glass; boron oxide, phosphor oxide, silicon oxide, and germanium oxide are the known formers in oxide glasses synthesized. Not only single–network former glasses, but

also double–network former glasses were investigated. Borosilicate glass is one of the double network former glasses. The interlinking of some borate and silicate networks is also possible with such glasses as reported by Axinte (2012). The modifier is an oxide of one of the transition metals, which is added to modifying properties of glass composition such as decreasing the melting point of the former. The intermediate is used to configure the links between the atomics of the glass composition.

2.3. Adsorbents (Oxide Glasses) synthesis

Conventional melt quenching is the technique used for oxide glasses synthesis. Three groups of oxide glasses were prepared: group I, group II, and group III. The chemical formula of group I is 45% GFO – 5% CuO – 5% Al_2O_3 – 45% Na_2O; where GFO (glass forming oxide) is B_2O_3 and SiO_2, labeled A and B respectively. The chemical formula of group II is 45% GFO – 5% Cu_2O – 5% Al_2O_3 – 45% Na_2O; GFO is B_2O_3 and SiO_2, labeled C and D respectively, this group tested to compare CuO and Cu_2O influence in adsorbent efficiency. Copper monoxide and dioxide were used as a modifier. The chemical formula of Hybrid borate and silicate (borosilicate) glasses (group III) is 25% B_2O_3–20% SiO_2 – 5% CuO – 5% GIO – 45% Na_2O; GIO (glass intermediating oxide) is Bi_2O_3, SnO, Al_2O_3 and, labeled I, J, K respectively, in order to find a better adsorbent. Table 1 summarizes the chemical composition of each system. Sodium carbonate is used as a precursor of Na_2O for reducing the melting point. The quantity of each chemical component in oxide glass composition was calculated based on its atomic weight by Eq. (1). All components of each oxide glass system were mixed and milled together in a porcelain mill, after determining the weight of each component for each oxide glass system. The porcelain crucible was used to contain the mixture, and then it was put in the furnace at 1000 ^oC for 60 min. Once the melt came out from the furnace to room temperature, the glass is formed as a piece with its properties. A grinding machine (Fritsch Mortar Automatic Grinder) was used to grind glass pieces to small particles size 125 - 63 µm.

$$Q_o = \frac{A.W * P\%}{F} \qquad Eq.(1)$$

Where: Q_o is the quantity of oxide by grams, A.W is the atomic weight of each component, P is the percentage of the component in glass composition. F is a factor used to make component value applicable. The amorphous structure of the prepared glasses was confirmed by X-Ray Diffraction instrumental techniques (XRD) and Fourier-transform infrared spectroscopy (FTIR), as well as ensures the existing of all chemicals used in the composition after melting process as mentioned by Sayyed et al. (2019). Furthermore, Brunauer–Emmett–Teller (BET) was used to define the surface area and pore radius as reported by Ouyang et al. (2020).

Table 1 Chemical Composition of Each System

System label	Glass chemical composition
A	45% B_2O_3 – 5% CuO – 5% Al_2O_3 – 45% Na_2O
B	45% SiO_2 – 5% CuO – 5% Al_2O_3 – 45% Na_2O
C	45% B_2O_3 – 5% Cu_2O – 5% Al_2O_3 – 45% Na_2O
D	45% SiO_2 – 5% Cu_2O – 5% Al_2O_3 – 45% Na_2O
I	25% B_2O_3–20% SiO_2 – 5% CuO – 5% Bi_2O_3 – 45% Na_2O
J	25% B_2O_3–20% SiO_2 – 5% CuO – 5% SnO – 45% Na_2O
K	25% B_2O_3–20% SiO_2 – 5% CuO – 5% AL_2O_3 – 45% Na_2O

2.4. Adsorption process

The adsorption efficiency of hardness removal on adsorbent (oxide glass types) is tested in experimental work, and then investigates the influence of experimental boundary conditions such as contact time, temperature, and adsorbent dosage, and the influence of the wastewater sample properties such as initial hardness concentration and pH value. In the first step of experimental work, the adsorbent dosage was 7.5 g L^{-1}, and it was added to the wastewater sample. Then magnetic stirrer used to stir the mixture at 300 rpm for 30 min at 40°C. Buchner funnel used to filter the mixture after the stirring step, and qualitative filter paper by size 0.45µm pore used in the filtration step. The filtrate was kept at 5°C to analysis time after the filtration step. The spectrophotometer (HACH DR6000) used for hardness value determination. Figure 1 summarizes experimental setup steps.

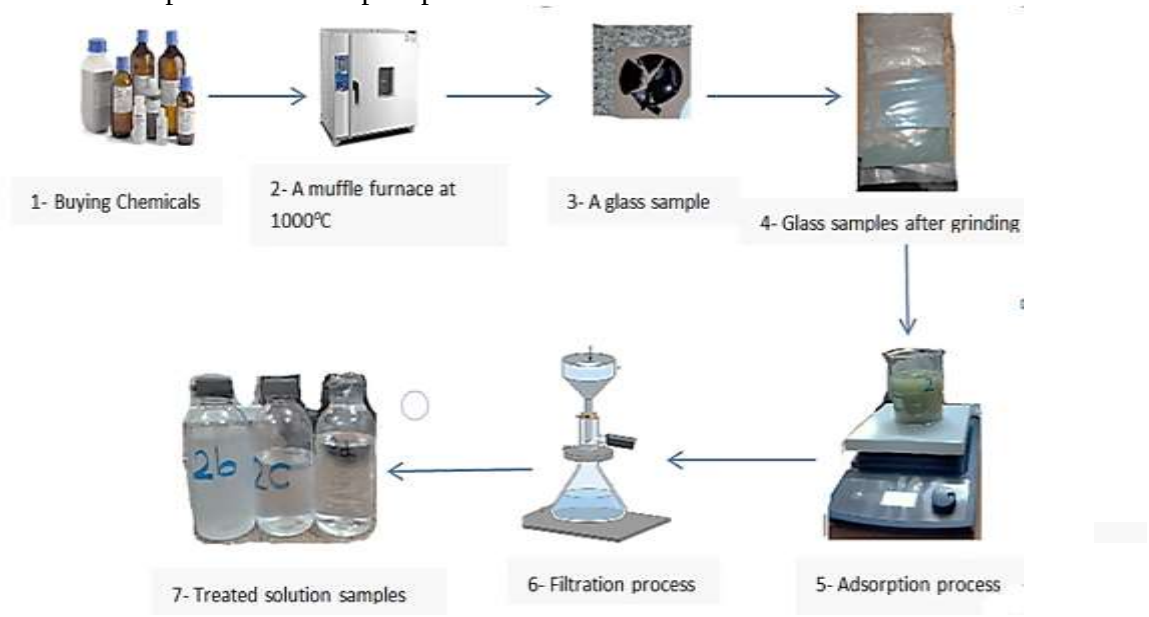

.

Fig. 1 Summarization of experimental setup steps

Oxide glass hardness removal efficiency (E) by percent and the adsorption capacity (Q_t) were calculated by Eq. (2) and (3) respectively:

$$E = 100\ \frac{C_0 - C_f}{C_o} \qquad Eq.(2)$$

$$Q_t = \frac{C_0 - C_t}{V} / m \qquad Eq.(3)$$

Where: C_o is the initial concentration of hardness ($mg_H\ L^{-1}$), C_t is the concentration of hardness ion ($mg_H\ L^{-1}$) at time t, C_f is the final concentrations of hardness ion ($mg_H\ L^{-1}$), V is the volume of wastewater sample (L), m is the adsorbent (oxide glass) mass (g), and Q_t is adsorption capacity of hardness ion per gram of oxide glass ($mg_H\ g_G^{-1}$) at a time t.

3.Results and Discussions

3.1. Characterizations of oxide glass adsorbents

3.1.1 XRD analysis

Oxide glasses (adsorbents) were investigated by X-Ray Diffraction instrumental techniques (XRD). Bucker D8 Advance Diffractometer was used in the two theta range from 10 to 80

degrees. The XRD patterns of oxide glasses are illustrated in Figure 2. It is observed that no crystalline peaks appear in all XRD patterns, indicating the amorphous nature of all glasses.

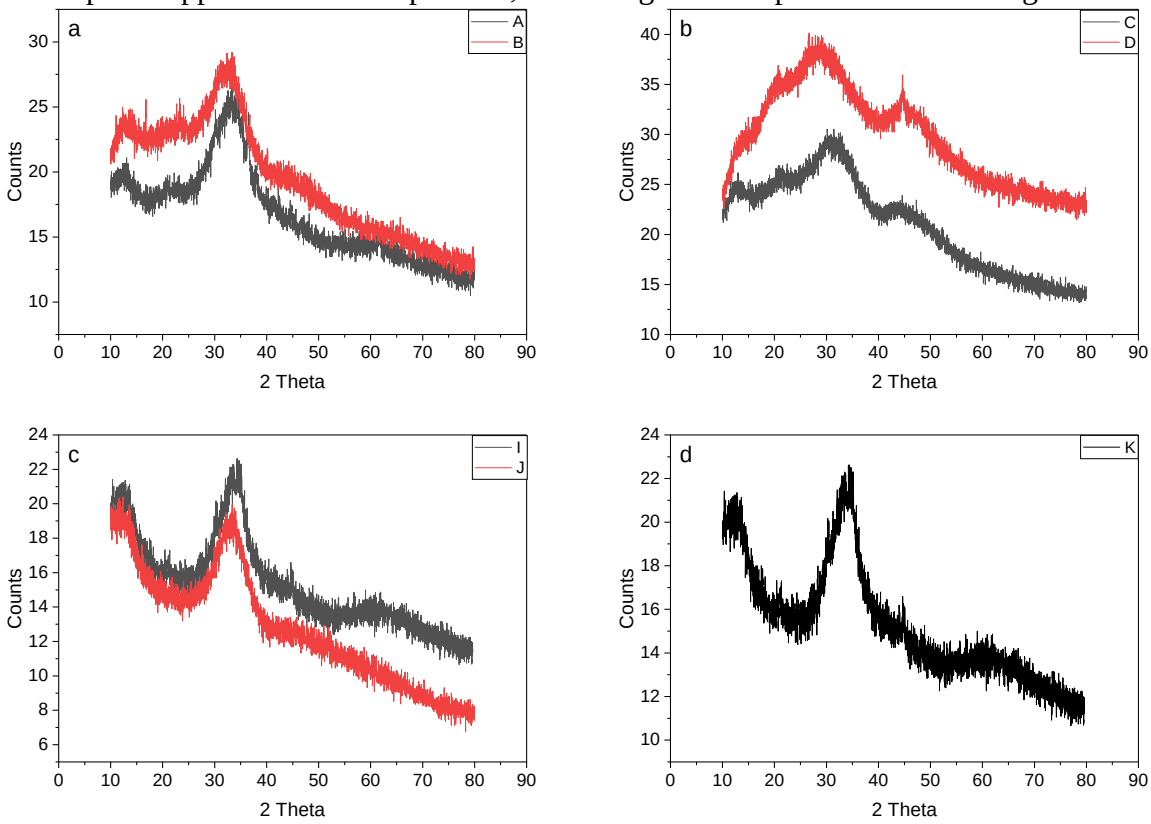

Fig. 2 X-ray powder diffraction for different oxide glass types (adsorbents: A, B, C, D, I, J, and K)

3.1.2 FTIR analysis

Borate, silicate, and borosilicate glasses were investigated by Fourier-transform infrared spectroscopy (FTIR). Platinum – ATR (Bruker Alpha) was used in the wavenumber range of 450–4000 cm^{-1}. The IR of borate glasses are illustrated in Figure 3. The absorption peaks of main IR in B_2O_3 containing glasses reside at wavenumbers of 710, 1260, and 1420 cm^{-1}. Feller and Kasper (1987) reported that the absorption peak near 1420 cm^{-1} appeared according to the groups boroxol ring stretching, and the 1260 cm^{-1} vibration is according to the B–O–B bond formation the linkage of boroxol groups to neighboring groups. The absorption band of bending vibrations of BO_3 triangles appears near 700 cm^{-1}, and stretching vibrations of BO_3 units with nonbridging oxygens (NBOs) appears the absorption band near 1380 cm^{-1} (Ardelean and Toderaş, 2006; Hartman and Chan, 1993; Krogh-Moe, 1965). B–O stretching of trigonal BO_3 units of vibrations 1200–1500 cm^{-1} , and B–O stretching of tetrahedral BO_4^- units of vibrations 850–1200 cm^{-1}, and 600–800 cm^{-1} is due to bonding vibrations of B–O–B groups in different borate segments (Gautam et al., 2012; Jellison and Bray, 1978).

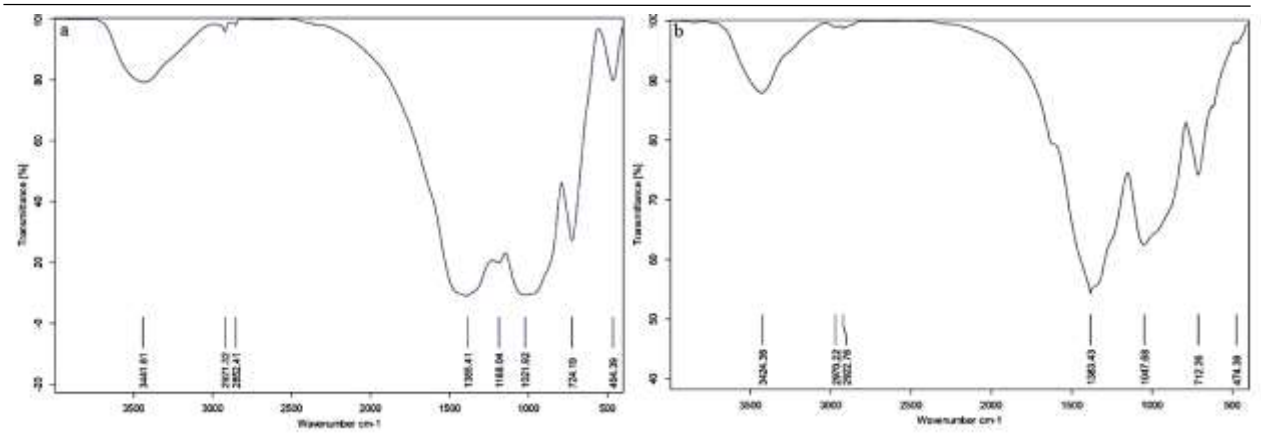

Fig. 3 FTIR spectrum for borate glasses a): sample A doped CuO, b): sample C doped Cu_2O

The IR spectra for silicate glass doped CuO (Figure 4a) had a wide and intense band at 878.51–989.17 cm^{-1} connected with the Si-O (ν_3 (Si-O)) asymmetric stretching vibrations in the SiO_4 tetrahedral groups lie in the silicates, and another at 460–470 cm^{-1} due to the ν_4 (O-Si-O) bending vibrations in the SiO_4 groups, and 695.03 cm^{-1} assigned to (ν (Si-O)) in the SiO_4 tetrahedron. The IR spectra for silicate glass doped Cu_2O (Figure 4b) had IR bands assignment similar to assignment of IR bands on the spectrum for silicate glass doped CuO as in the silicates, but with the occurrence of minor displacements in the wavenumbers of bands, where the modifier used is copper (I) oxide (Aktas et al., 2016; Torres-Carrasco et al., 2014).

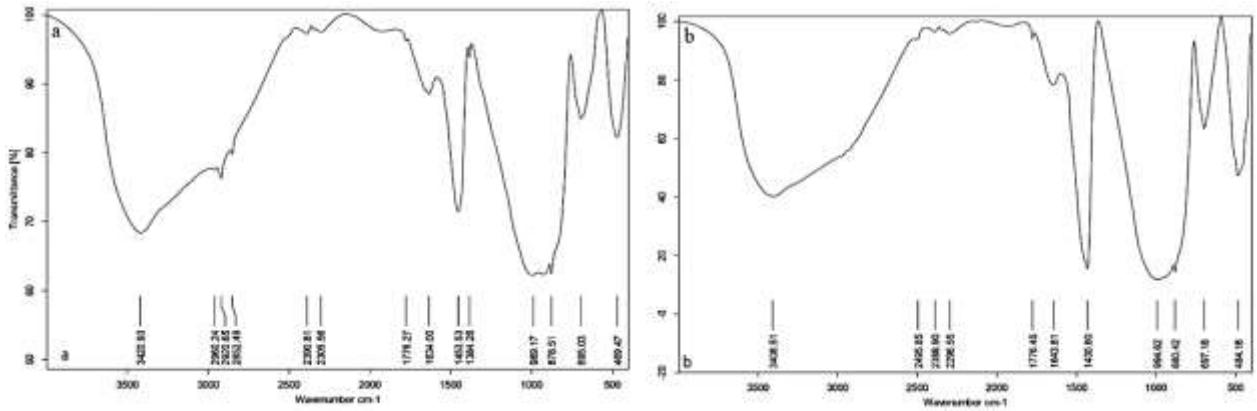

Fig. 4 FTIR spectrum for silicate glasses, a): sample B doped CuO, b): sample D doped Cu_2O

Figure 5a shows the IR spectra for borosilicate glass sample K. The bending vibration peak of Si–O–Si lies at 473.5 cm^{-1}, and the stretching vibration peak of O–Si–O near 800 cm^{-1}. The absorption peak near 1187.26 cm^{-1} is the bending vibration peak of Si–O–Si, which synchronizes with the stretching vibration peak of BO_4 (antisymmetric). In addition, the absorption peaks near 725.35 cm^{-1} and 1450.35 cm^{-1} are bending vibration peak of BO_3 and anti-symmetric stretching vibration peak of BO_3, respectively (X. Li et al., 2018). Theoretically, when adding a small amount of Al_2O_3 into borosilicate glass, Al^{3+} has priority to attract free oxygen to form [AlO_4], accessing the structure of SiO_2 to achieve the more stable structure (X. Li et al., 2018). Further, due to the oxygen deficiency, B^{3+} essentially exists in the form of [BO_3] instead of [BO_4]. In Figure 5b and 5c, the same peaks mentioned are achieved in the case of the borosilicate glass with Bi_2O_3 and SnO respectively, but with slight shifts in the wavenumbers as a result of the use of another glass intermediating oxide.

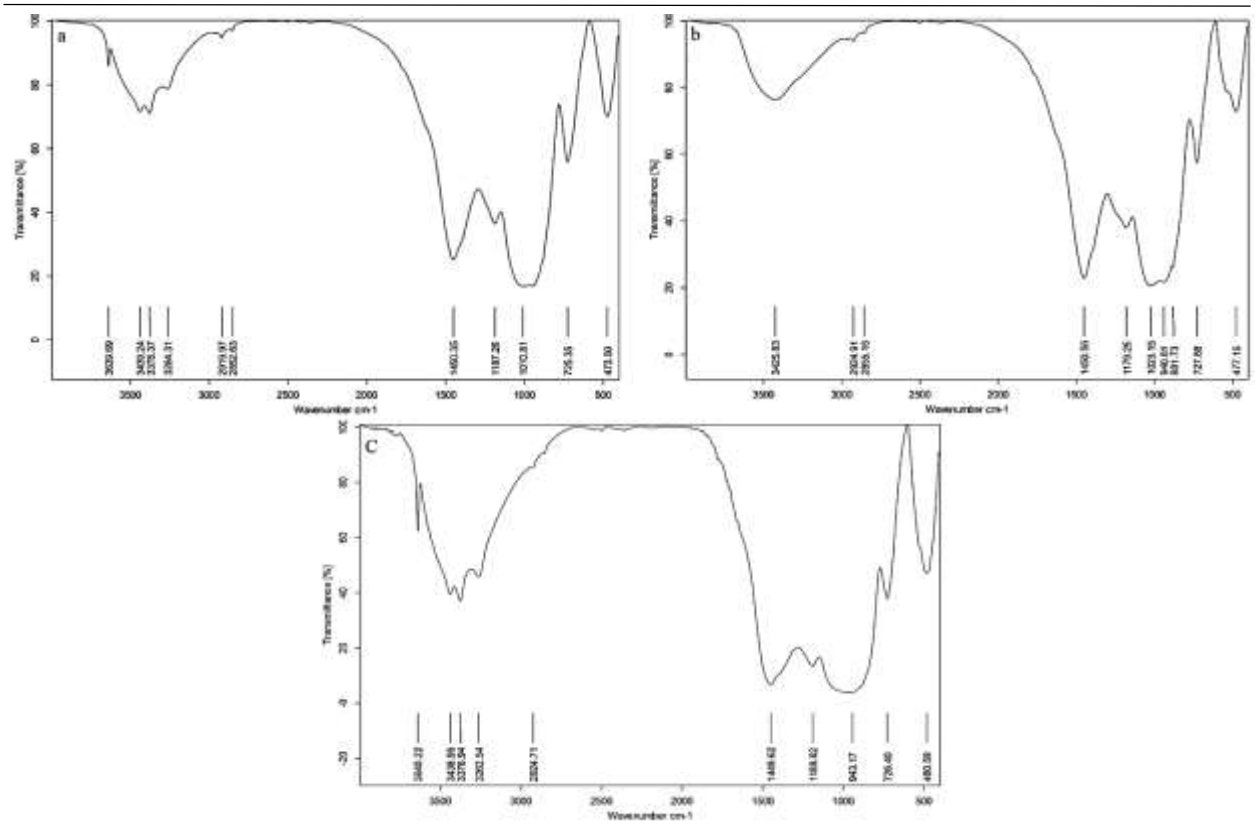

Fig. 5 FTIR spectrum for borosilicate glasses, a): sample K, b): sample I, c): sample J

3.1.3 BET Analysis

The surface area and pore size of oxide glasses (adsorbents) were investigated by Brunauer–Emmet–Teller (BET). Nova touch LX^4 Quantachrome instrument version 1.21 was used to measure the surface area and average pore radius of oxide glass samples in powder case.
The results are illustrated in Table 2.

Table 2 The Surface Area and Average Pore Radius of Oxide Glass Samples (BET Analysis)

Oxide Glass	Surface Area	average pore radius
	$m^2 g^{-1}$	nm
A	22.78	1.83
B	30.78	1.35
C	23.70	1.34
D	25.61	1.20
I	29.84	1.80
J	45.69	1.56
K	18.57	1.60

Determining the surface area and pore size of the adsorbents are extremely important because of their impact on the efficiency of the adsorption process. The surface area indicates the availability of active sites, which receiving atoms or molecules of adsorbate. The surface area can be controlled by controlling the size of the adsorbent particles, when the size of the adsorbent particles is minimized through the grinding process, the surface area increases for the same amount of adsorbent, that leads to improve the efficiency of the adsorption process (Ahn et al.,

2008; Hwang et al., 2011; Mossa Hosseini et al., 2011). Therefore, the pore size of adsorbent and its arrangement, both have a significant impact on efficiency of adsorption process. Pore size controls if molecules of adsorbate can enter to them, where adsorbate molecules can be adsorbed in the pores of adsorbent molecules, which have size larger than molecules of adsorbate as reported by W. Li et al. (2019). As for the arrangement of the pores, Suresh Kumar et al. (2019) reported that it has an effect on the one hand if they present as long isolated cylinders or they are highly branched.

3.2. Influence of oxide glass composition

Influence of oxide glass chemical composition on hardness removal efficiency is shown in Figure 6. The calcium ions removal efficiency with adsorbents A, B, C, and D is around 36%, 37%, 31%, and 11% respectively, and the magnesium ions removal efficiency with adsorbents A, B, C, and D is around 35%, 28%, 33%, and 7% respectively. It's observed that the hardness removal efficiency of samples A and B is approximately similar; the hardness removal efficiency of sample C is close to A and B, as shown in Figure 6a. The efficiency of sample D in removing hardness is the lowest and with a large difference. Therefore, the modifier Cu_2O was dispensed, which has a weak improvement effect on hardness removal efficiency in case of borate glass and significant decrease in case of silicate glass. Hence, the decision was made to prepare a glass system with merge boron oxide and silicone oxide in one chemical composition.

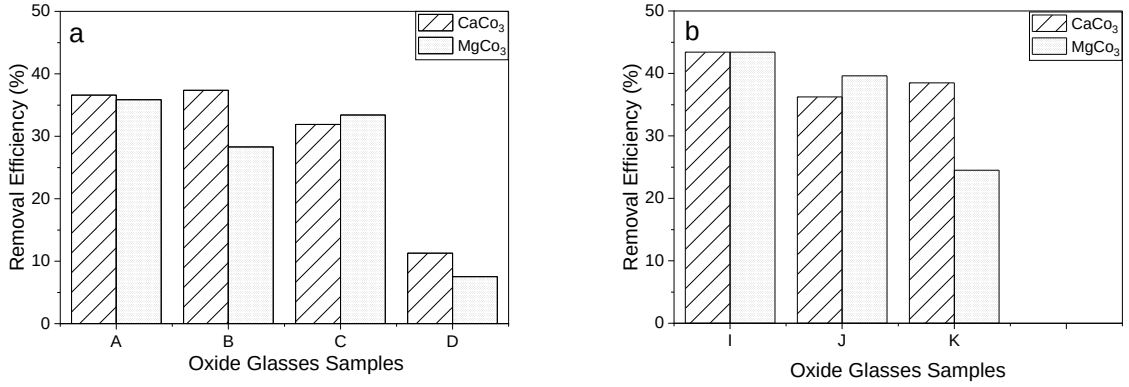

Fig. 6 Ca^{2+} and Mg^{2+} Removal Efficiency of oxide glass types, a): borate and silicate glass samples, b): borosilicate glass samples

This explains the reason for the desirable using CuO as a modifier in the oxide glass system at the next step. Based on the results, the formers used for the next stages were boron oxide and silicone oxide. Boron and silicon oxide together are the formers with modifier CuO to investigate intermediate types.

Figure 6b shows the hardness removal efficiencies of samples I, J, and K; they have the same chemical composition except for the intermediate oxide. Oxide glass sample I gives the best hardness removal efficiency, which contains Bi_2O_3 as intermediate oxide, bearing in mind that the differences between the hardness removal efficiency are small, the calcium ions removal efficiency with adsorbents I, J and K is around 43%, 36%, and 38% respectively, and the magnesium ions removal efficiency with adsorbents I, J and K is around 43%, 39%, and 24% respectively. And by reviewing Table 2, which displays the specific surface area and pore radius of adsorbents, it was found that the increase in surface area of adsorbent is not necessary to improve the adsorption efficiency, also the pore diameter as long as the adsorbents are different in chemical composition as reported by Santoso et al. (2020). The efficiency of adsorption process depends on several factors, not only the surface area and pore size of adsorbent but also

the surface charge of adsorbent and adsorbate has a significant effect, but in the case of using the same adsorbent, the specific surface area has an important role, as mentioned in previous studies, which presented the decreasing of adsorbent particles size leads to increase the surface area of adsorbent, which in turn enhances the quantity of active sites and thus increases the efficiency of adsorption process (Baral et al., 2007; Imchuen et al., 2016; Y. Wang et al., 2006). In this study the comparison is between more than one adsorbent, which have different characteristics and chemical composition. The surface area of an adsorbent may be larger than another, but the surface charge of adsorbent and adsorbate is an important factor to achieve the attraction and increase adsorption capacity (Garg et al., 2015; Liu et al., 2014), which is affected by pH value (Mahmoodi and Saffar-Dastgerdi, 2019; Olusegun et al., 2018). Adsorbent chemical composition, as the interactions between oxides to composite the oxide glass sample, it can create electrostatic interferences for instance the electrical surface charges on the oxide glass particles, which increase or decrease the attraction between the adsorbed in wastewater sample and the surfaces of the oxide glass particles (Malamis and Katsou, 2013). Moreover, the molar volume of adsorbate may be larger than the pore radius of adsorbent, which leads to difficulty in completing the adsorption process for this adsorbent, as the pores size and its arrangement has a significant effect on possibility of contaminants molecules accessing to the inner part of adsorbent (W. Li et al., 2019; Ouyang et al., 2020; Suresh Kumar et al., 2019). All this indicates that the adsorption process depends on the nature of adsorbent and adsorbate.

3.3. Influence of Boundary conditions

As the type of used adsorbent is important, boundary conditions of experimental work are no less important than it, to achieve the superiority of the adsorption process. Some boundary conditions were studied in this work and their influence on the adsorption process performance.

3.3.1 Contact time

Three types of oxide borosilicate glass I, J, and K were examined in five periods of contact time: (30, 60, 90, 120, and 150 min). Studies were done in same value of conditions as following: adsorbent dosage 7.5 g L^{-1}, pH 8.9, initial concentration of total hardness 319 ± ٧ mg L^{-1}, and temperature 40 ^{o}C. Periods of contact time were measured and set by minutes. The performance of adsorbents in hardness removal at different contact times is illustrated in Figure 7.

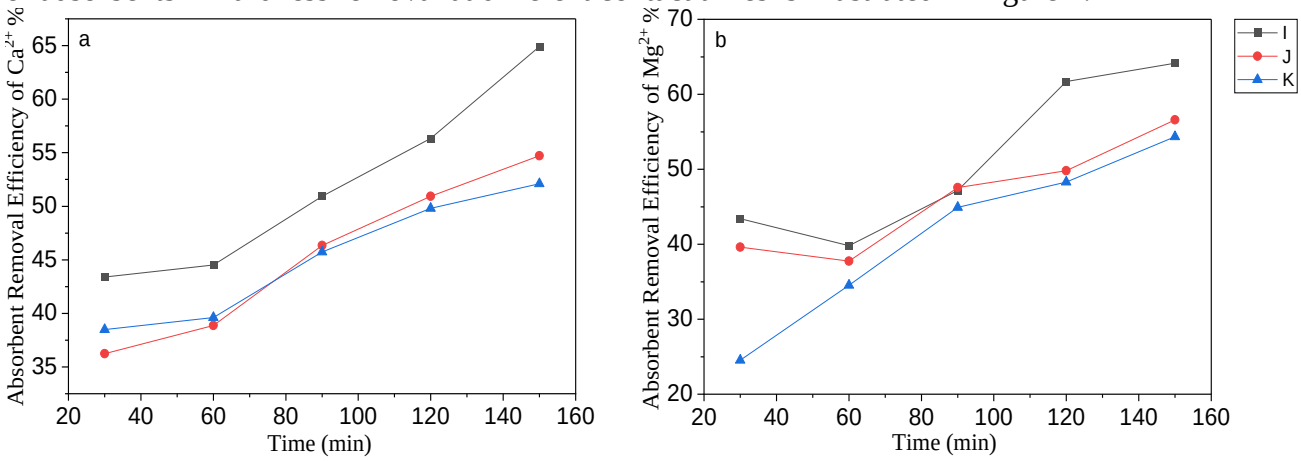

Fig. 7 Influence of contact time on adsorbents removal efficiency (a): Ca^{2+} and (b): Mg^{2+}

As observed, the efficiency of three adsorbents in the minimization of hardness was amended by increasing the contact time. Adsorbent I with intermediate Bi_2O_3 achieved the best removal

efficiency of total hardness over the duration of the adsorption process. The removal efficiencies of Ca^{2+} and Mg^{2+} with adsorbent I at 30 min are around 43%, then they are increasing over time to be around 64% in 150 min. The removal efficiencies of Ca^{2+} and Mg^{2+} with adsorbent J at 30 min are around 36% and 39% respectively; these at 150 min are around 54% and 56% respectively. The removal efficiencies of Ca^{2+} and Mg^{2+} with adsorbent K at 30 min are around 38% and 24% respectively; these at 150 min are around 52% and 54% respectively. In general, with increasing the contact time, more active sites were occupied achieving its maximum capacity as mentioned by Ashour et al. (2017). There is high increase in removal efficiency was observed at the initial phases of contact time because of the availability of active sites for the adsorption process, and the adsorption process tends to equilibrium gradually as reported by Qin et al. (2010).

The results from the contact time study were analyzed by Langmuir and Freundlich isothermal adsorption models. Langmuir theory supports that the adsorption process is monolayer adsorption (Eq. (4)) (Langmuir, 1917), it is based on assumptions

1- Dynamic equilibrium (rate of desorption is the same of adsorption rate at equilibrium point)
2- The surface of adsorbent material is homogenous
3- Neglect the interaction between the adsorbate molecules and adsorbent surface

$$\frac{C_e}{Q_e} = \frac{1}{K_{eq}} + \frac{C_e}{Q_{max}} \qquad Eq.(4)$$

Freundlich theory supports that the adsorbent surface isn't homogenous (Eq. (5)) (Gawande et al., 2017). The theory works on the assumption that adsorption sites of the adsorbent surface have different adsorption energy.

$$\log Q_e = \log K_F + \frac{1}{n}\log C_e \qquad Eq.(5)$$

The parameter K_{eq} is Langmuir constant; the parameters K_F, n are Freundlich constants; C_e is the adsorbate concentration at equilibrium adsorption (mg L^{-1}); Q_e is the adsorption capacity at equilibrium adsorption (mg g^{-1}); Q_{max} is the maximum adsorption capacity (mg g^{-1}).
The adsorption isotherm data were reported in Table 3, and they were illustrated in Figures 8 and 9.

Table 3 Fitted Parameters Determined for The Adsorption Isotherms.

Adsorbate		Langmuir model, Eq. (4)			Freundlich model, Eq. (5)		
		K_{eq} (L mg^{-1})	Q_{max} (mg g^{-1})	R^2	K_F	n	R^2
Ca^{2+}	I	0.177	9.88	0.98	1.07	1.18	0.98
	J	0.088	7.0	0.99	6.43	0.83	0.99
	K	0.088	7.04	0.99	6.8	0.82	0.99
Mg^{2+}	I	0.16	1.86	0.99	0.64	1.11	0.99
	J	0.099	1.49	0.98	1.42	0.88	0.98
	K	0.048	0.95	0.95	6.19	0.63	0.96

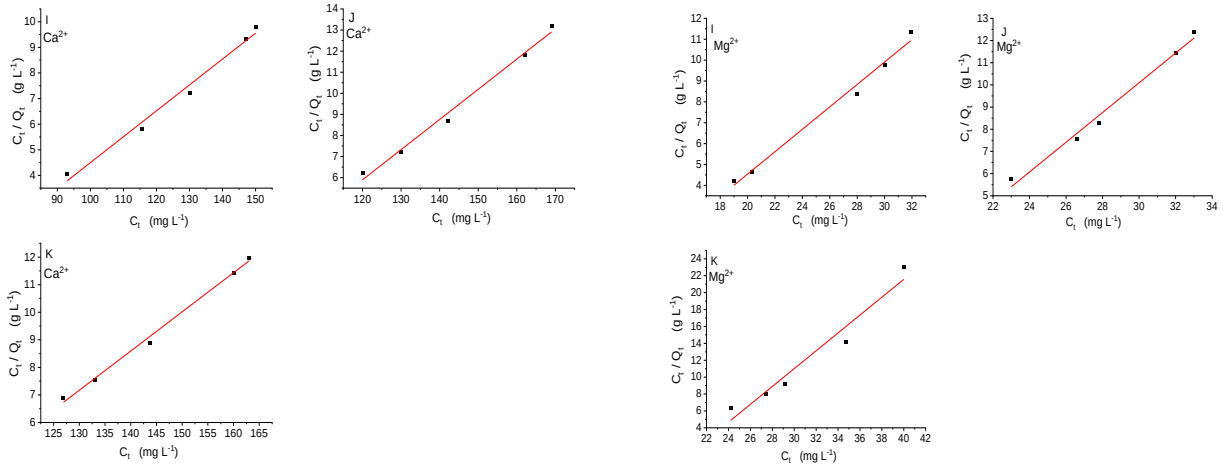

Fig. 8 Linear plot of Langmuir isotherm of Ca^{2+} and Mg^{2+} on adsorbens I, J, and K

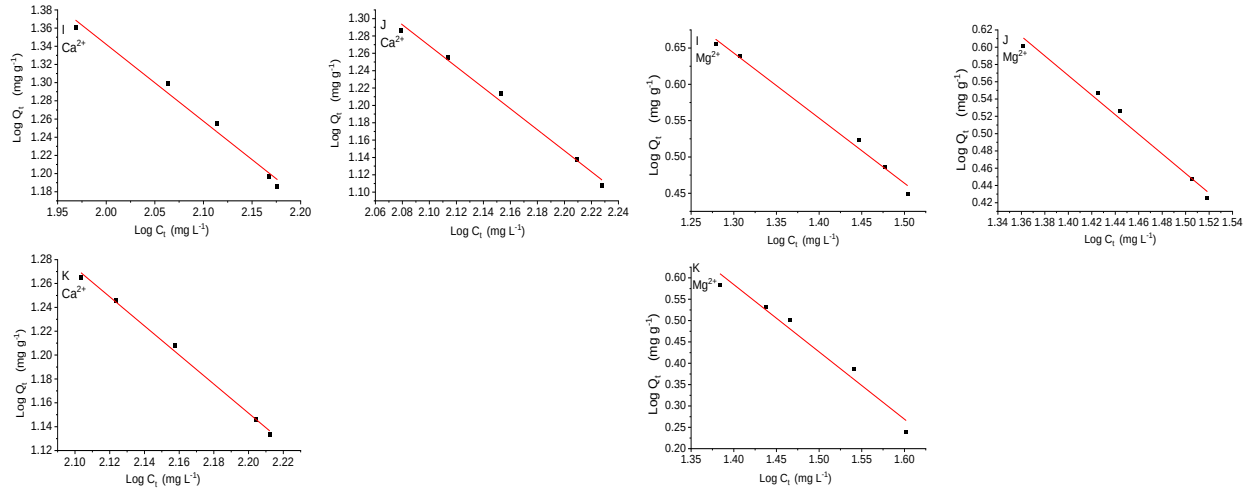

Fig. 9 Linear plot of Freundlich isotherm of Ca^{2+} and Mg^{2+} on adsorbents I, J, and K

As shown in Figures 8 and 9, and Table 3, the conclusions from the Langmuir and Freundlich graphic relations model well fitted with both isothermal adsorption models. That means the adsorption process can be carried out chemically or physically for the three borosilicate glasses.

3.3.2 Temperature:

The influence of temperature in range of 30 – 70 ^{o}C was investigated; its results were illustrated in Figure 10. The process was conducted under boundary condition as follow: contact time of 150 min and adsorbent dosage of 7.5 g L^{-1}, and the characteristics of the wastewater samples are, pH value of 8.9, initial concentration of total hardness 319 ± ٧ mg L^{-1}. Figure 10 shows the semi constant behavior of hardness adsorption with increasing temperature in most cases, and even an increase in removal efficiency in some cases isn't noteworthy compared to the cost of temperature increase. That means the influence of temperature can be negligible in the hardness removal efficiency of tested adsorbents in the range studied, these results matched with what have been published in some previous studies (El-Nahas et al., 2020; Lodeiro et al., 2006; Rolence, 2014; Sanjuán et al., 2019; Sepehr et al., 2013a). Adsorbent I removal efficiency of Ca^{2+} and Mg^{2+} is in the range around 64 – 65% and 63 – 65% respectively, adsorbent J removal

efficiency of Ca^{2+} and Mg^{2+} is in the range around 54 – 55% and 56 – 57% respectively, and adsorbent k removal efficiency of Ca^{2+} and Mg^{2+} is in the range around 51 – 52% and 54 – 57% respectively, at temperature degree from 30 to 70 ^{o}C. Then ambient temperature can consider as acceptable temperature for the removal of total hardness using this technique without affecting efficiency.

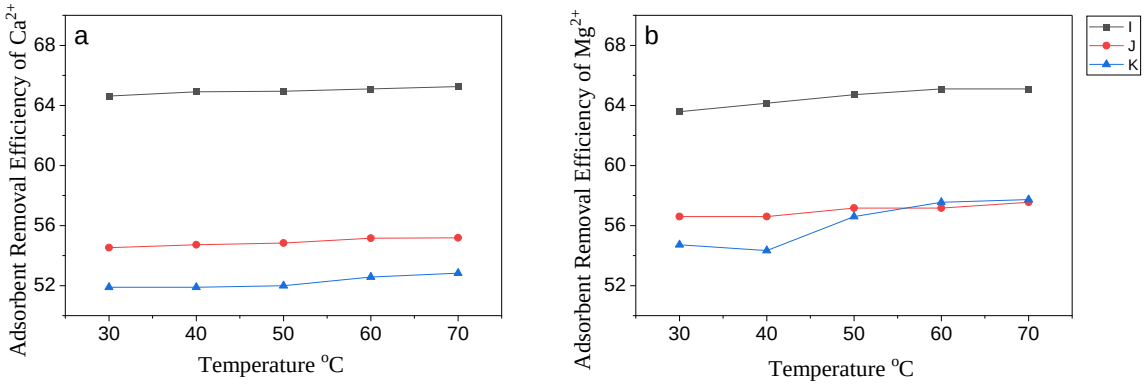

Fig. 10 Influence of temperature on adsorbents removal efficiency (a): Ca^{2+} and (b): Mg^{2+}

3.3.3 Adsorbent Dosage:

The influence of adsorbent dosage in range of 2.5 – 15 g L^{-1} was examined in adsorption of total hardness; at contact time 150 min, pH 8.9, initial concentration of total hardness 319 ± ٧ mg L^{-1}, and temperature 40 ^{o}C. The results were illustrated in Figure 11.

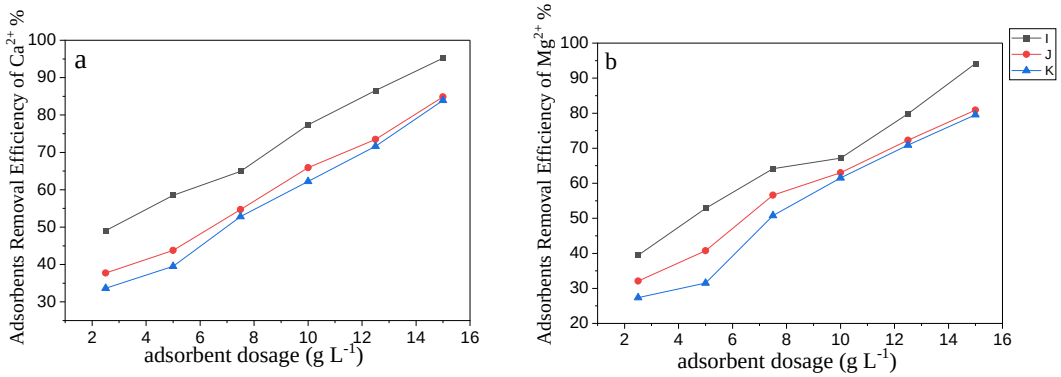

Fig.11 Influence of adsorbent dosage on adsorbents removal efficiency (a): Ca^{2+} and (b): Mg^{2+}

As seen in Figure 11 removal efficiencies of Ca^{2+} and Mg^{2+} are improving with adsorbent dosage increases, that attributed to the availability of more active sites with increasing adsorption surface area by adsorbent dosage increase. In the case of adsorbent I, removal efficiencies of Ca^{2+} and Mg^{2+} are around 49% and 39% respectively with an adsorbent dosage of 2.5g L^{-1}. Removal efficiencies of Ca^{2+} and Mg^{2+} with adsorbent I increase to around 95% and 94% respectively with an adsorbent dosage of 15 g L^{-1}. The same behavior was observed with adsorbents J and K but with lower performance than adsorbent I. In the case of adsorbent J, removal efficiencies of Ca^{2+} and Mg^{2+} are around 37% and 32% respectively with an adsorbent dosage of 2.5g L^{-1}, then these increase to around 85% and 81% respectively with an adsorbent dosage of 15 g L^{-1}. In the case of adsorbent K, removal efficiencies of Ca^{2+} and Mg^{2+} are around 33% and 27% respectively with an adsorbent dosage of 2.5g L^{-1}, then these increase to around 84% and 80% respectively with an adsorbent dosage of 15 g L^{-1}. The previous notes mean the occupied sites of adsorbent I is greater

than the occupied sites of adsorbents J and K, and the adsorption process improves with the adsorbent dosage increasing, as this allows the presence of active sites in a larger quantity to accommodate the hardness ions. Previous studies reported the same behavior with increasing removal efficiency with adsorbent dosage; they pointed that attributed to adsorption increasing following the increase dosage of adsorbent due to availability of adsorbent active sites (Das and Das, 2013; Esposito et al., 2001; Xie et al., 2015).

3.4 Influence of wastewater Properties

3.4.1 Initial hardness concentration

The influence of the initial hardness concentrations was studied, that in the case of initial concentration of total hardness from 50 : 318 mg L^{-1} and pH value 8.9, and boundary conditions: contact time 150 min, adsorbent dosage 7.5g L^{-1}, and temperature 40°C. The results are illustrated in Figure 12. As it is observed, adsorption efficiency was improved by increasing the initial hardness concentration from 50: 150 mg L^{-1}, and then adsorption efficiency was decreased by increasing the initial hardness concentration from 150: 318 mg L^{-1}.

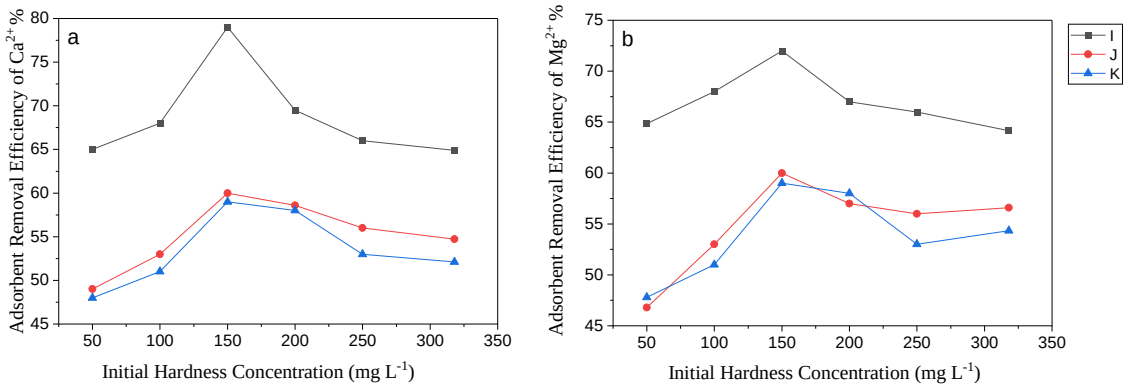

Fig. 12 Influence of initial hardness concentration on adsorbents removal efficiency (a): Ca^{2+} and (b): Mg^{2+}

As Figure 12a shows, in the case of the initial hardness concentration is 50 mg L^{-1}, the removal efficiency of Ca^{2+} is around 65%, 47%, and 48% for adsorbents I, J, and K respectively. The removal efficiency of Ca^{2+} is increasing with increasing the initial hardness concentration, which reaches around 79%, 60%, and 59% with a hardness concentration of 150 mg L^{-1}. The removal efficiency of Ca^{2+} start to decrease with increasing the initial hardness concentration from 150 mg L^{-1} to 318 mg L^{-1}, as it is around 64%, 54%, and 52% for adsorbents I, J, and K respectively with initial hardness concentration of 318 mg L^{-1}. The same behavior was observed with Mg^{2+} removal efficiency in Figure 12b. At the initial hardness concentration 50 mg L^{-1}, removal efficiency is around 64%, 46%, and 47% for adsorbents I, J, and K respectively, and then this reaches around 73%, 60%, and 58% with hardness concentration 150 mg L^{-1}. Then the removal efficiency of Mg^{2+} decreases with initial hardness increasing, as it is around 64%, 56%, and 54% for adsorbents I, J, and K respectively with an initial hardness concentration 318 mg L^{-1}. In case of low hardness concentrations, the ions might be attracted to active sites of adsorbent. At the increasing of ions concentrations, more ions have the capability to occupy active sites. That refers to the differences in the mechanism of ion adsorption, ion adsorption is subjected to adsorbent pores, paths of the arranged lattice, and the need for interchangeable cations' displacement (Arancibia-Miranda et al., 2016; Es et al., 2019; Farrag et al., 2017). The results confirm that excessive initial hardness concentration leads to increase in the adsorbent capacity to adsorb but to a certain limit. If it is considered that surface adsorption is the ion removal driving force that

means increasing the initial concentration of Ca^{2+} and Mg^{2+} leads to improve the driving force (Payus et al., 2019; Sepehr et al., 2013a). After an initial hardness concentration of 150 mg L^{-1}, the removal efficiency for Ca^{2+} and Mg^{2+} decreases with the initial hardness concentration increasing, which indicates the active sites for adsorbent, it is no longer sufficient to accommodate the same proportion from the initial hardness concentration. Thus, the adsorption efficiency of the adsorbent decreases because of active sites occupied with Ca^{2+} and Mg^{2+} cations (Kyzioł-Komosińska et al., 2015; Lee and Rees, 1987; Sanjuán et al., 2019).

3.4.2 pH value:

The pH of the sample has an important influence on the contaminants' adsorption processes as reported by Mahmoodi and Saffar-Dastgerdi (2019), as that effect contaminants' ionization and the adsorbent surface charge. The influence of pH on the removal efficiency of glasses was investigated from 4.1 to 11 at a contact time of 150 min, adsorbent dosage of 7.5 g L^{-1}, and temperature 40^{o}C, the initial hardness concentration for wastewater samples was 319±ٰ mg L^{-1}. The pH was controlled by adding 0.1M NaOH or 0.1M HCl solution and measuring by a pH meter (JENWAY 3510). As observed in Figure 13, the removal efficiency percentage of Ca^{2+} and Mg^{2+} with adsorbent I increases from around 49% to 93% and from around 47% to 91% with increasing pH from 4.1 to 6.5 respectively, and then these percentages decrease from around 92% to 49% and from around 88% to 47% with increasing pH from 7.2 to 11 respectively. The same behavior appeared with adsorbents J and K, the removal efficiency percentage of Ca^{2+} increases with adsorbent J from around 44% to 85%, and with adsorbent K from around 42% to 84% with increasing pH from 4.1 to 6.5 respectively. Then the removal efficiency percentage of Ca^{2+} decreases with adsorbent J from around 84% to 39% and with adsorbent K from around 82% to 36% with increasing pH from 7.2 to 11 respectively, and the same case is in the removal efficiency percentage of Mg^{2+}. That is attributed to the high level of removed proton of the functional group on the hydrogen bond surface, which happens in case of high pH as mentioned by Aragaw and Ayalew (2019). The best removal efficiencies of oxide glasses I, J, and K were achieved at pH range 6.5 – 7.2, which is close to the range reported by Barathi et al. (2014), as the adsorbent surface has a negative charge and the adsorbate cations have a positive charge, this is due to the effect of the pH value on a adsorbent surface charge as reported by Olusegun et al. (2018). The weak adsorption capacity at an acidic medium (from 4.1 – 5.3) is due to ion exchange proton in functional groups or contest of H^{+} with ions of metals to fill the active sites of the oxide glasses (Iqbal et al., 2009; F. T. Li et al., 2007; Saeed et al., 2005). As for the alkaline media (from pH 8.9 – 11), Lodeiro et al. (2006) believe that the metal hydroxide formation mainly causes the metal adsorption decrease as it is low-soluble.

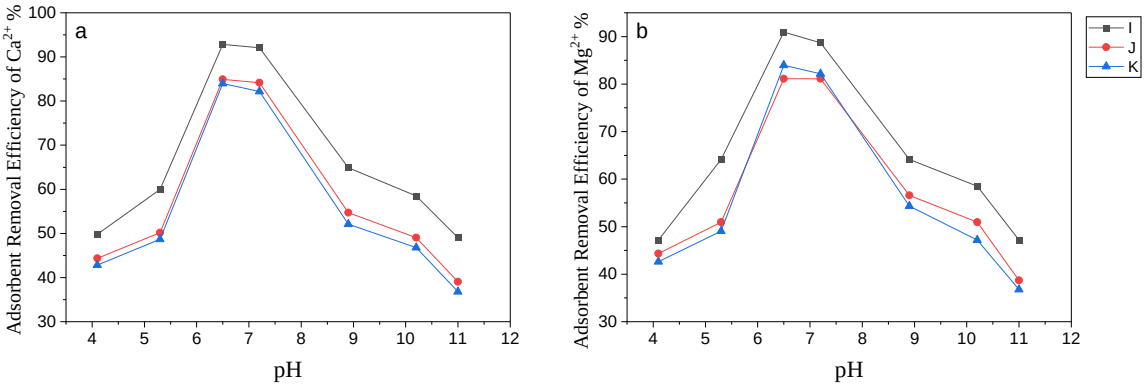

Fig. 13 Influence of pH value on adsorbents removal efficiency (a): Ca^{2+} and (b): Mg^{2+}

The comparison between various adsorbents in hardness removal efficiency is shown in table 4. Among the previous studies on various absorbents, the borosilicate glass I in the current study has shown acceptable hardness removal efficiency, that at appropriate contact time and adsorbent dosage.

Table 4 Comparison of Hardness Removal Efficiency of Borosilicate Glass (I) with Other Adsorbents.

Adsorbent (Reference)	Removal efficiency	Contact time	Hardness initial concentration	adsorbent dosage	pH
zeolite synthesized from Ethiopian kaolin (Aragaw and Ayalew, 2019)	94.1% Ca^{2+}, 81.4% Mg^{2+}	150 min	1000 mg L^{-1}	5 g L^{-1}	6.5
nano powder zeolite (El-Nahas et al., 2020)	90 % Ca^{2+}, Mg^{2+}	30 min	>1000 mg L^{-1}	10 g L^{-1}	**NA**
modified bentonite (Kadir et al., 2017)	6.67% Ca^{2+}, Mg^{2+}	75 min	120 mg L^{-1}	**NA**	**NA**
pine nut cover (Kaur et al., 2021)	90.44% Ca^{2+}	15 min	680 mg L^{-1}	6 g L^{-1}	6-7
Coffee ground activated charcoal (Khaerul and Syahputri, 2021)	97.8 % Ca^{2+}	75 min	565.17 mg L^{-1}	10 g L^{-1}	7
Nano-zeolite-graphene oxide composite (Konale et al., 2020)	98% Ca^{2+}	120 min	250 mg L^{-1}	1 g L^{-1}	7
Coconut shell activated carbons (Rolence, 2014)	60 %	10 h	655 mg L^{-1}	240 g L^{-1}	6.3
Natural zeolite (Hailu et al., 2019)	79.9% Ca^{2+}, 85.6% Mg^{2+}	30 min	658 mg L^{-1} (TH)	50 g L^{-1}	6.9
Amberlite 748 (Yu et al., 2009)	**NA**	8 h	100 mg L^{-1}	120 mg L^{-1}	9.5
Kaolinite smectile (Es et al., 2019)	98.24% Ca^{2+}, 99.24% Mg^{2+}	30 min	100 mg L^{-1}	1 g L^{-1}	8
Coconut shell powder (Tomar, 2018)	62.58 %	3 h	890 mg L^{-1}	6 g L^{-1}	7
Neem leaves (Tomar, 2018)	59.52 %	3 h	420 mg L^{-1}	2 g L^{-1}	7
Modified pumice (Sepehr et al., 2013b)	61% Ca^{2+}, 51% Mg^{2+}	240 min	150 mg L^{-1}	6 g L^{-1}	6
Borosilicate glass I (current study)	93% Ca^{2+}, 91% Mg^{2+}	150 min	319±٧ mg L^{-1}	7.5 g L^{-1}	6.5

* **NA** refers to no available information.

4. Conclusions

The results of this research referred to that borosilicate glass achieved noticeable success in adsorption process, especially sample (I). Hardness removal efficiency increases with increasing contact time from contact time 30 min to 150 min. The conclusions from the Langmuir and Freundlich graphic relations model well fitted with both isothermal adsorption models. That means the hardness adsorption process can be carried out chemically or physically for three borosilicate glasses. The improvement of hardness removal efficiency is slight and not noticeable with increasing temperature, that in range of tested temperature from 30 – 70 ºC. The adsorption process efficiency increases with increasing the adsorbent dosage, at the range of tested dosage

from 2.5 g L^{-1} to 15 g L^{-1}. Adsorption process performance is variable with increasing the initial hardness concentration, hardness ions removal efficiency increases in case of increasing the initial hardness concentration from 50 to 150 mg L^{-1}, then it decreases with increasing the initial hardness concentration from 150 to 318 mg L^{-1}. Adsorption process performance achieves to its best case at pH value range (6.5 – 7.2). As a conclusion, the optimum boundary conditions for enhancing removal efficiency of total hardness from industrial wastewater using borosilicate glass type I (B_2O_3 +SiO_2 as former, and CuO as modifier, with intermediate Bi_2O_3) as adsorbent are; 150 min contact time, and adsorbent dosage 15 g L^{-1}, with the initial hardness concentration equal to 150 mg L^{-1}, and pH range 6.5 – 7.2 for wastewater properties. It is recommend further investigation to identify the influence of use other oxides as a modifier or others as intermediate, in addition to study the influence of sample (I) on other contaminants in wastewater.

Declarations:

Ethical approval

This article does not contain any studies with human participants or animals performed by any authors.

Competing interests

The authors declare they have no competing interests.

Acknowledgments

This research was funded by Science Technology and Innovation Funding Authority (STDF) under grant Post Graduate Support Grant (PGSG). https://stdf.eg/web/grants/open .

References

Ahn, M. K., Chilakala, R., Han, C., and Thenepalli, T. (2018). Removal of hardness fromwater samples by a carbonation process with a closed pressure reactor. *Water (Switzerland)*, *10*(1), 1–10. https://doi.org/10.3390/w10010054

Ahn, S. C., Oh, S. Y., and Cha, D. K. (2008). Enhanced reduction of nitrate by zero-valent iron at elevated temperatures. *Journal of Hazardous Materials*, *156*(1–3), 17–22. https://doi.org/10.1016/j.jhazmat.2007.11.104

Aktas, B., Albaskar, M., Yalcin, S., and Dogru, K. (2016). Optical properties of soda-lime-silica glasses doped with peanut shell powder. *Archives of Materials Science and Engineering*, *82*(2), 57–61. https://doi.org/10.5604/01.3001.0009.7104

Ambaye, T. G., Vaccari, M., van Hullebusch, E. D., Amrane, A., and Rtimi, S. (2021). Mechanisms and adsorption capacities of biochar for the removal of organic and inorganic pollutants from industrial wastewater. *International Journal of Environmental Science and Technology*, *18*(10), 3273–3294. https://doi.org/10.1007/s13762-020-03060-w

Anesthesia, N., Be, S., In, M. O., In, L., Appropriate, W., Equipment, R., Are, D., Available, I., Manage, T. O., Ii, G., By, I., With, A. P., Privileges, A., By, M., Under, O. R., Medical, T. H. E., Iii, G., Has, P., Examined, B., … Complications, O. (2010). Guidelines for. In *Resuscitation*.

APHA. (2002). American Public Health Association; American Water Works Association; Water Environment Federation. *Standard Methods for the Examination of Water and Wastewater*, *02*, 1–541.

Aragaw, T. A., and Ayalew, A. A. (2019). Removal of water hardness using zeolite synthesized

from Ethiopian kaolin by hydrothermal method. *Water Practice and Technology*, *14*(1), 145–159. https://doi.org/10.2166/wpt.2018.116

Arancibia-Miranda, N., Baltazar, S. E., García, A., Muñoz-Lira, D., Sepúlveda, P., Rubio, M. A., and Altbir, D. (2016). Nanoscale zero valent supported by Zeolite and Montmorillonite: Template effect of the removal of lead ion from an aqueous solution. *Journal of Hazardous Materials*, *301*, 371–380. https://doi.org/10.1016/j.jhazmat.2015.09.007

Ardelean, I., and Toderaş, M. (2006). FTIR structural investigation of 3B2O3-BaO glass matrix containing manganese ions. *Journal of Optoelectronics and Advanced Materials*, *8*(3), 1118–1120.

Ashour, R. M., Abdelhamid, H. N., Abdel-Magied, A. F., Abdel-Khalek, A. A., Ali, M. M., Uheida, A., Muhammed, M., Zou, X., and Dutta, J. (2017). Rare Earth Ions Adsorption onto Graphene Oxide Nanosheets. *Solvent Extraction and Ion Exchange*, *35*(2), 91–103. https://doi.org/10.1080/07366299.2017.1287509

Axinte, E. (2011). Glasses as engineering materials: A review. *Materials and Design*, *32*(4), 1717–1732. https://doi.org/10.1016/j.matdes.2010.11.057

Axinte, E. (2012). Metallic glasses from " alchemy" to pure science: Present and future of design, processing and applications of glassy metals. *Materials and Design*, *35*, 518–556. https://doi.org/10.1016/j.matdes.2011.09.028

Baral, S. S., Das, S. N., Rath, P., and Chaudhury, G. R. (2007). Chromium(VI) removal by calcined bauxite. *Biochemical Engineering Journal*, *34*(1), 69–75. https://doi.org/10.1016/j.bej.2006.11.019

Barathi, M., Krishna Kumar, A. S., Kumar, C. U., and Rajesh, N. (2014). Graphene oxide-aluminium oxyhydroxide interaction and its application for the effective adsorption of fluoride. *RSC Advances*, *4*(96), 53711–53721. https://doi.org/10.1039/c4ra10006a

Bouassida, M., Fourati, N., Ghazala, I., Ellouze-Chaabouni, S., and Ghribi, D. (2018). Potential application of Bacillus subtilis SPB1 biosurfactants in laundry detergent formulations: Compatibility study with detergent ingredients and washing performance. *Engineering in Life Sciences*, *18*(1), 70–77. https://doi.org/10.1002/elsc.201700152

Camilo, M. E., Silva, E. D. O., De Assumpção, T. A. A., Kassab, L. R. P., and De Araújo, C. B. (2013). White light generation in Tm3+/Ho3+/Yb3+ doped PbO-GeO2 glasses excited at 980 nm. *Journal of Applied Physics*, *114*(16), 3–7. https://doi.org/10.1063/1.4827863

Crini, G., and Lichtfouse, E. (2019). Advantages and disadvantages of techniques used for wastewater treatment. *Environmental Chemistry Letters*, *17*(1), 145–155. https://doi.org/10.1007/s10311-018-0785-9

Das, N., and Das, D. (2013). Recovery of rare earth metals through biosorption: An overview. *Journal of Rare Earths*, *31*(10), 933–943. https://doi.org/10.1016/S1002-0721(13)60009-5

Decundo, J. M., Diéguez, S. N., Martínez, G., Romanelli, A., Fernández Paggi, M. B., Pérez Gaudio, D. S., Amanto, F. A., and Soraci, A. L. (2019). Impact of water hardness on oxytetracycline oral bioavailability in fed and fasted piglets. *Veterinary Medicine and Science*, *5*(4), 517–525. https://doi.org/10.1002/vms3.185

El-Nahas, S., Osman, A. I., Arafat, A. S., Al-Muhtaseb, A. H., and Salman, H. M. (2020). Facile and affordable synthetic route of nano powder zeolite and its application in fast softening of

water hardness. *Journal of Water Process Engineering*, *33*(November 2019), 101104. https://doi.org/10.1016/j.jwpe.2019.101104

Es, S., Fathy, M., Im, E., Sa, A., and Shehata, N. (2019). *International Journal of Chemical Effective Solutions of Hardness by Using Adsorption Technique on Kaolinite Smectite Adsorbent from Aqueous Solution*. *202*, 1–13.

Esposito, A., Pagnanelli, F., Lodi, A., Solisio, C., and Vegliò, F. (2001). Biosorption of heavy metals by Sphaerotilus natans: An equilibrium study at different pH and biomass concentrations. *Hydrometallurgy*, *60*(2), 129–141. https://doi.org/10.1016/S0304-386X(00)00195-X

Farrag, A. E. H. A., Abdel Moghny, T., Mohamed, A. M. G., Saleem, S. S., and Fathy, M. (2017). Abu Zenima synthetic zeolite for removing iron and manganese from Assiut governorate groundwater, Egypt. *Applied Water Science*, *7*(6), 3087–3094. https://doi.org/10.1007/s13201-016-0435-y

Federation, W. E. (1999). Standard Methods for the Examination of Water and Wastewater Standard Methods for the Examination of Water and Wastewater. *Public Health*, *51*(1), 940–940. https://doi.org/10.2105/AJPH.51.6.940-a

Feller, S., and Kasper, J. E. (1987). *Steve FELLER,*. *91*, 324–332.

Garg, A., Mainrai, M., Bulasara, V. K., and Barman, S. (2015). Experimental investigation on adsorption of amido black 10b dye onto zeolite synthesized from fly ash. *Chemical Engineering Communications*, *202*(1), 123–130. https://doi.org/10.1080/00986445.2013.836636

Gautam, C., Yadav, A. K., and Singh, A. K. (2012). A Review on Infrared Spectroscopy of Borate Glasses with Effects of Different Additives. *ISRN Ceramics*, *2012*, 1–17. https://doi.org/10.5402/2012/428497

Gawande, S. M., Belwalkar, N. S., and Mane, A. A. (2017). Adsorption and its Isotherm – Theory. *International Journal of Engineering Research*, *6*(6), 312. https://doi.org/10.5958/2319-6890.2017.00026.5

Hailu, Y., Tilahun, E., Brhane, A., Resky, H., and Sahu, O. (2019). Ion exchanges process for calcium, magnesium and total hardness from ground water with natural zeolite. *Groundwater for Sustainable Development*, *8*, 457–467. https://doi.org/10.1016/j.gsd.2019.01.009

Halpegama, J. U., Heenkenda, K. Y., Wu, Z., Nanayakkara, K. G. N., Rajapakse, R. M. G., Bandara, A., Herath, A. C., Chen, X., and Weerasooriya, R. (2021). Concurrent removal of hardness and fluoride in water by monopolar electrocoagulation. *Journal of Environmental Chemical Engineering*, *9*(5), 106105. https://doi.org/10.1016/j.jece.2021.106105

Hartman, P., and Chan, H. K. (1993). Application of the Periodic Bond Chain (PBC) Theory and Attachment Energy Consideration to Derive the Crystal Morphology of Hexamethylmelamine. *Pharmaceutical Research: An Official Journal of the American Association of Pharmaceutical Scientists*, *10*(7), 1052–1058. https://doi.org/10.1023/A:1018927109487

Hwang, Y. H., Kim, D. G., and Shin, H. S. (2011). Mechanism study of nitrate reduction by nano zero valent iron. *Journal of Hazardous Materials*, *185*(2–3), 1513–1521.

https://doi.org/10.1016/j.jhazmat.2010.10.078

Imchuen, N., Lubphoo, Y., Chyan, J. M., Padungthon, S., and Liao, C. H. (2016). Using cation exchange resin for ammonium removal as part of sequential process for nitrate reduction by nanoiron. *Sustainable Environment Research*, *26*(4), 156–160. https://doi.org/10.1016/j.serj.2016.01.002

Iqbal, M., Saeed, A., and Zafar, S. I. (2009). FTIR spectrophotometry, kinetics and adsorption isotherms modeling, ion exchange, and EDX analysis for understanding the mechanism of Cd2+ and Pb2+ removal by mango peel waste. *Journal of Hazardous Materials*, *164*(1), 161–171. https://doi.org/10.1016/j.jhazmat.2008.07.141

Jabbar-Lopez, Z. K., Ung, C. Y., Alexander, H., Gurung, N., Chalmers, J., Danby, S., Cork, M. J., Peacock, J. L., and Flohr, C. (2021). The effect of water hardness on atopic eczema, skin barrier function: A systematic review, meta-analysis. *Clinical and Experimental Allergy*, *51*(3), 430–451. https://doi.org/10.1111/cea.13797

Jamilatun, S., and Mufandi, I. (2020). The Effectiveness of Activated Charcoal from Coconut Shell as The Adsorbent of Water Purification in The Laboratory Process of Chemical Engineering Universitas Ahmad Dahlan Yogyakarta. *Jurnal Teknik Kimia Dan Lingkungan*, *4*(2), 113. https://doi.org/10.33795/jtkl.v4i2.151

Jellison, G. E., and Bray, P. J. (1978). A structural interpretation of B10 and B11 NMR spectra in sodium borate glasses. *Journal of Non-Crystalline Solids*, *29*(2), 187–206. https://doi.org/10.1016/0022-3093(78)90113-8

Jiménez, J. A., Sendova, M., Liu, H., and Fernandez, F. E. (2011). Supersaturation-Driven Optical Tuning of Ag Nanocomposite Glasses for Photonics: An In Situ Optical Microspectroscopy Study. *Plasmonics*, *6*(2), 399–405. https://doi.org/10.1007/s11468-011-9217-4

Kadir, N. N. A., Shahadat, M., and Ismail, S. (2017). Formulation study for softening of hard water using surfactant modified bentonite adsorbent coating. *Applied Clay Science*, *137*, 168–175. https://doi.org/10.1016/j.clay.2016.12.025

Kaur, C., Roy, T., Das, S., Gupta, R., and Pramanik, T. (2021). Preparation and application of bio-adsorbent for the removal of water hardness: conversion of a waste to a value-added material. *Biomass Conversion and Biorefinery*, *0123456789*. https://doi.org/10.1007/s13399-021-01806-1

Khaerul, A., and Syahputri, Y. (2021). *COFFEE GROUND ACTIVATED CHARCOAL AND ITS POTENTIAL AS AN ADSORBENT OF Ca 2 + AND Mg 2 + IONS IN REDUCING WATER HARDNESS*. *01*(02), 42–45.

Konale, R. A., Mahale, N. K., and Ingle, S. T. (2020). Nano-zeolite-graphene oxide composite for calcium hardness removal: Isotherm and kinetic study. *Water Practice and Technology*, *15*(4), 1011–1031. https://doi.org/10.2166/wpt.2020.079

Kozisek, F. (2020). Regulations for calcium, magnesium or hardness in drinking water in the European Union member states. *Regulatory Toxicology and Pharmacology*, *112*(January), 104589. https://doi.org/10.1016/j.yrtph.2020.104589

Krogh-Moe, J. (1965). The crystal structure of silver tetraborate Ag 2 O.4B 2 O 3 . *Acta Crystallographica*, *18*(1), 77–81. https://doi.org/10.1107/s0365110x65000142

Kyzioł-Komosińska, J., Rosik-Dulewska, C., Franus, M., Antoszczyszyn-Szpicka, P., Czupioł, J., and Krzyżewska, I. (2015). Sorption capacities of natural and synthetic zeolites for Cu(II) ions. *Polish Journal of Environmental Studies*, *24*(3), 1111–1123. https://doi.org/10.15244/pjoes/30923

Langmuir, I. (1917). The constitution and fundamental properties of solids and liquids. *Journal of the Franklin Institute*, *183*(1), 102–105. https://doi.org/10.1016/S0016-0032(17)90938-X

Lee, E. F. T., and Rees, L. V. C. (1987). Dealumination of sodium Y zeolite with hydrochloric acid. *Journal of the Chemical Society, Faraday Transactions 1: Physical Chemistry in Condensed Phases*, *83*(5), 1531–1537. https://doi.org/10.1039/F19878301531

Li, F. T., Yang, H., Zhao, Y., and Xu, R. (2007). Novel modified pectin for heavy metal adsorption. *Chinese Chemical Letters*, *18*(3), 325–328. https://doi.org/10.1016/j.cclet.2007.01.034

Li, W., Mu, B., and Yang, Y. (2019). Feasibility of industrial-scale treatment of dye wastewater via bio-adsorption technology. *Bioresource Technology*, *277*, 157–170. https://doi.org/10.1016/j.biortech.2019.01.002

Li, X., Feng, J., Jiang, Y., Lin, H., and Feng, J. (2018). Preparation and anti-oxidation performance of Al2O3-containing TaSi2-MoSi2-borosilicate glass coating on porous SiCO ceramic composites for thermal protection. *RSC Advances*, *8*(24), 13178–13185. https://doi.org/10.1039/c8ra00703a

Liu, S., Ding, Y., Li, P., Diao, K., Tan, X., Lei, F., Zhan, Y., Li, Q., Huang, B., and Huang, Z. (2014). Adsorption of the anionic dye Congo red from aqueous solution onto natural zeolites modified with N,N-dimethyl dehydroabietylamine oxide. *Chemical Engineering Journal*, *248*, 135–144. https://doi.org/10.1016/j.cej.2014.03.026

Lodeiro, P., Barriada, J. L., Herrero, R., and Sastre de Vicente, M. E. (2006). The marine macroalga Cystoseira baccata as biosorbent for cadmium(II) and lead(II) removal: Kinetic and equilibrium studies. *Environmental Pollution*, *142*(2), 264–273. https://doi.org/10.1016/j.envpol.2005.10.001

Mahmoodi, N. M., and Saffar-Dastgerdi, M. H. (2019). Zeolite nanoparticle as a superior adsorbent with high capacity: Synthesis, surface modification and pollutant adsorption ability from wastewater. *Microchemical Journal*, *145*(August 2018), 74–83. https://doi.org/10.1016/j.microc.2018.10.018

Mahyudin, D. (2019). *Banana Stem Charcoal as Adsorbents Reduce Water Hardness Levels*. *1*(1), 1–6.

Malamis, S., and Katsou, E. (2013). A review on zinc and nickel adsorption on natural and modified zeolite, bentonite and vermiculite: Examination of process parameters, kinetics and isotherms. *Journal of Hazardous Materials*, *252–253*, 428–461. https://doi.org/10.1016/j.jhazmat.2013.03.024

Mgombezi, D., and Vegi, M. R. (2020). *An Investigation on Effectiveness of Grafted Potato Starch as an Adsorbent for Hard Water Treatment*. *2020*.

Mossa Hosseini, S., Ataie-Ashtiani, B., and Kholghi, M. (2011). Nitrate reduction by nano-Fe/Cu particles in packed column. *Desalination*, *276*(1–3), 214–221. https://doi.org/10.1016/j.desal.2011.03.051

Naghsh, M., and Shams, K. (2017). Synthesis of a kaolin-based geopolymer using a novel fusion method and its application in effective water softening. *Applied Clay Science*, *146*(March), 238–245. https://doi.org/10.1016/j.clay.2017.06.008

Of, O., Use, T., Carbon, C. B. A., and Water, H. (2022). *The Use of Coconut-Shell Based Activated Carbon as an Adsorbent in the Treatment of Hard Water*. *M*(2009).

Olusegun, S. J., de Sousa Lima, L. F., and Mohallem, N. D. S. (2018). Enhancement of adsorption capacity of clay through spray drying and surface modification process for wastewater treatment. *Chemical Engineering Journal*, *334*(November 2017), 1719–1728. https://doi.org/10.1016/j.cej.2017.11.084

Ouyang, J., Zhou, L., Liu, Z., Heng, J. Y. Y., and Chen, W. (2020). Biomass-derived activated carbons for the removal of pharmaceutical mircopollutants from wastewater: A review. *Separation and Purification Technology*, *253*(June), 117536. https://doi.org/10.1016/j.seppur.2020.117536

Payus, C. M., Refdin, M. A., Zahari, N. Z., Rimba, A. B., Geetha, M., Saroj, C., Gasparatos, A., Fukushi, K., and Alvin Oliver, P. (2019). Durian husk wastes as low-cost adsorbent for physical pollutants removal: Groundwater supply. *Materials Today: Proceedings*, *42*(xxxx), 80–87. https://doi.org/10.1016/j.matpr.2020.10.006

Qin, C., Wang, R., and Ma, W. (2010). Adsorption kinetic studies of calcium ions onto Ca-Selective zeolite. *Desalination*, *259*(1–3), 156–160. https://doi.org/10.1016/j.desal.2010.04.015

Rapant, S., Cvečková, V., Fajčíková, K., Sedláková, D., and Stehlíková, B. (2017). Impact of calcium and magnesium in groundwater and drinking water on the health of inhabitants of the Slovak Republic. *International Journal of Environmental Research and Public Health*, *14*(3). https://doi.org/10.3390/ijerph14030278

Rolence, C. (2014). Water Hardness Removal by Coconut Shell Activated Carbon. *International Journal of Science, Technology and Society*, *2*(5), 97. https://doi.org/10.11648/j.ijsts.20140205.11

Saeed, A., Iqbal, M., and Akhtar, M. W. (2005). Removal and recovery of lead(II) from single and multimetal (Cd, Cu, Ni, Zn) solutions by crop milling waste (black gram husk). *Journal of Hazardous Materials*, *117*(1), 65–73. https://doi.org/10.1016/j.jhazmat.2004.09.008

Sanjuán, I., Benavente, D., Expósito, E., and Montiel, V. (2019). Electrochemical water softening: Influence of water composition on the precipitation behaviour. *Separation and Purification Technology*, *211*(October 2018), 857–865. https://doi.org/10.1016/j.seppur.2018.10.044

Santoso, E., Ediati, R., Kusumawati, Y., Bahruji, H., Sulistiono, D. O., and Prasetyoko, D. (2020). Review on recent advances of carbon based adsorbent for methylene blue removal from waste water. *Materials Today Chemistry*, *16*, 100233. https://doi.org/10.1016/j.mtchem.2019.100233

Sayyed, M. I., Kaky, K. M., Gaikwad, D. K., Agar, O., Gawai, U. P., and Baki, S. O. (2019). Physical, structural, optical and gamma radiation shielding properties of borate glasses containing heavy metals (Bi 2 O 3 /MoO 3). *Journal of Non-Crystalline Solids*, *507*(December 2018), 30–37. https://doi.org/10.1016/j.jnoncrysol.2018.12.010

Sepehr, M. N., Zarrabi, M., Kazemian, H., Amrane, A., Yaghmaian, K., and Ghaffari, H. R. (2013a). Removal of hardness agents, calcium and magnesium, by natural and alkaline modified pumice stones in single and binary systems. *Applied Surface Science*, *274*, 295–305. https://doi.org/10.1016/j.apsusc.2013.03.042

Sepehr, M. N., Zarrabi, M., Kazemian, H., Amrane, A., Yaghmaian, K., and Ghaffari, H. R. (2013b). Removal of hardness agents, calcium and magnesium, by natural and alkaline modified pumice stones in single and binary systems. *Applied Surface Science*, *274*, 295–305. https://doi.org/10.1016/j.apsusc.2013.03.042

Shahedi, A., Darban, A. K., Taghipour, F., and Jamshidi-Zanjani, A. (2020). A review on industrial wastewater treatment via electrocoagulation processes. *Current Opinion in Electrochemistry*, *22*, 154–169. https://doi.org/10.1016/j.coelec.2020.05.009

Sharmin, S., Mia, J., Miah, M. S., and Zakir, H. M. (2020). Hydrogeochemistry and heavy metal contamination in groundwaters of Dhaka metropolitan city, Bangladesh: Assessment of human health impact. *HydroResearch*, *3*, 106–117. https://doi.org/10.1016/j.hydres.2020.10.003

Sun, N., Zhou, H., Zhang, H., Zhang, Y., Zhao, H., and Wang, G. (2021). Synchronous removal of tetracycline and water hardness ions by capacitive deionization. *Journal of Cleaner Production*, *316*(November 2020), 128251. https://doi.org/10.1016/j.jclepro.2021.128251

Suresh Kumar, P., Korving, L., Keesman, K. J., van Loosdrecht, M. C. M., and Witkamp, G. J. (2019). Effect of pore size distribution and particle size of porous metal oxides on phosphate adsorption capacity and kinetics. *Chemical Engineering Journal*, *358*(July 2018), 160–169. https://doi.org/10.1016/j.cej.2018.09.202

Suzuki, K., Tanaka, Y., Osada, T., and Waki, M. (2002). Removal of phosphate, magnesium and calcium from swine wastewater through crystallization enhanced by aeration. *Water Research*, *36*(12), 2991–2998. https://doi.org/10.1016/S0043-1354(01)00536-X

Takahashi, Y., and Imaizumi, Y. (1988). Hardness in Drinking Water. *Eisei Kagaku*, *34*(5), 475–479. https://doi.org/10.1248/jhs1956.34.475

Tomar, Y. S. (2018). Removal of Chloride, Hardness and TDS from Water Using Different Adsorbents. *International Journal for Research in Applied Science and Engineering Technology*, *6*(4), 5111–5117. https://doi.org/10.22214/ijraset.2018.4834

Torfs, E., Nopens, I., Winkler, M., Vanrolleghem, P., Balemans, S., and Smets, I. (2016). *Experimental Methods in Wastewater Treatment, (Chapter6:Settling Tests)*.

Torres-Carrasco, M., Palomo, J. G., and Puertas, F. (2014). Sodium silicate solutions from dissolution of glasswastes. Statistical analysis. *Materiales de Construccion*, *64*(314). https://doi.org/10.3989/mc.2014.05213

Vedishcheva, N. M., and Wright, A. C. (2014). Chemical structure of oxide glasses: A concept for establishing structure-property relationships. In *Glass: Selected Properties and Crystallization* (Issue January 2014). https://doi.org/10.1515/9783110298581.269

Wahyuni, N., Zaharah, T. A., and Ria, R. (2021). Characterization of Hydrochloric Acid Activated Natural Kaolin and its application as adsorbent for Mg2+. *Journal of Physics: Conference Series*, *1882*(1). https://doi.org/10.1088/1742-6596/1882/1/012099

Wang, L., and Lin, S. (2019). Mechanism of Selective Ion Removal in Membrane Capacitive

Deionization for Water Softening. *Environmental Science and Technology*, *53*(10), 5797–5804. https://doi.org/10.1021/acs.est.9b00655

Wang, Y., Liu, S., Xu, Z., Han, T., Chuan, S., and Zhu, T. (2006). Ammonia removal from leachate solution using natural Chinese clinoptilolite. *Journal of Hazardous Materials*, *136*(3), 735–740. https://doi.org/10.1016/j.jhazmat.2006.01.002

Xie, J., Lin, Y., Li, C., Wu, D., and Kong, H. (2015). Removal and recovery of phosphate from water by activated aluminum oxide and lanthanum oxide. *Powder Technology*, *269*, 351–357. https://doi.org/10.1016/j.powtec.2014.09.024

Yadav, A. K., and Singh, P. (2015). A review of the structures of oxide glasses by Raman spectroscopy. *RSC Advances*, *5*(83), 67583–67609. https://doi.org/10.1039/c5ra13043c

Yan, M., Wang, D., Ni, J., Qu, J., Yan, Y., and Chow, C. W. K. (2008). Effect of polyaluminum chloride on enhanced softening for the typical organic-polluted high hardness North-China surface waters. *Separation and Purification Technology*, *62*(2), 401–406. https://doi.org/10.1016/j.seppur.2008.02.014

Yu, Z., Qi, T., Qu, J., Wang, L., and Chu, J. (2009). Removal of Ca(II) and Mg(II) from potassium chromate solution on Amberlite IRC 748 synthetic resin by ion exchange. *Journal of Hazardous Materials*, *167*(1–3), 406–412. https://doi.org/10.1016/j.jhazmat.2008.12.140

Zereffa, E. A., and Bekalo, T. B. (2017). Clay Ceramic Filter for Water Treatment. *Materials Science and Applied Chemistry*, *34*(1), 69–74. https://doi.org/10.1515/msac-2017-0011